

Response to the comments by Reviewers

We appreciate the efforts and comments the reviewers have made in the reviewing process of our paper. Thanks for the opportunity to revise our paper. As the reviewer suggested, we have removed R^2 from the objective function. Also we have corrected Equation (20) for the water balance error (WBE). We hope these changes have adequately addressed the reviewer's concern. Supplements include revised manuscript and response to the comments by reviewers.

Comments

The changes you have made to your manuscript based on reviewer comments have been well received by the reviewer. Only some remarks are being made: first is to remove R^2 as an objective function: please consider whether you wish to do so or not. If you would like to maintain its inclusion, then please add some concerns with respect to this objective function.

Response:

We agree with the reviewer. We have removed R^2 from the objective function. The revision has been made. We also update our paper such as descriptions of results and tables according to this change.

--Line 879-881.

Table 3 Summary results of the model calibration under different climatic conditions (*i.e.* dry and wet periods).

Indicator	SIMHYD	SIMHYD	DWBM	DWBM
	calibrated on dry period	calibrated on wet period	calibrated on dry period	calibrated on wet period
25th NSE	0.84	0.85	0.71	0.77
Median NSE	0.70	0.77	0.58	0.66
75th NSE	0.61	0.68	0.43	0.54
Average NSE	0.70	0.76	0.57	0.65
25th d_I	0.77	0.79	0.71	0.75
Median d_I	0.72	0.76	0.67	0.71
75th d_I	0.70	0.74	0.61	0.68
Average d_I	0.73	0.76	0.65	0.71
25th WBE	22	16	25	24
Median WBE	13	8	15	12
75th WBE	6	4	9	5
Average WBE	14	11	22	17

--Line 894-896.

Table 4 Summary results of the model validation when calibrated under different climatic conditions.

Model	Indicator	dry/dry	dry/wet	wet/dry	wet/wet	
SIMHYD	25th NSE	0.72	0.74	0.68	0.77	
	Median NSE	0.55	0.64	0.51	0.69	
	75th NSE	0.42	0.44	0.41	0.55	
	Average NSE	0.57	0.61	0.54	0.66	
	25th d_I	0.74	0.78	0.74	0.78	
	Median d_I	0.71	0.74	0.70	0.75	
	75th d_I	0.66	0.70	0.63	0.72	
	Average d_I	0.69	0.73	0.68	0.74	
	25th WBE	34	30	39	23	
	Median WBE	20	19	28	13	
	75th WBE	14	8	16	7	
	Average WBE	24	21	29	17	
	DWBM	25th NSE	0.56	0.65	0.51	0.72
		Median NSE	0.46	0.48	0.45	0.61
		75th NSE	0.34	0.35	0.30	0.42
		Average NSE	0.48	0.52	0.45	0.59
25th d_I		0.69	0.73	0.68	0.74	
Median d_I		0.65	0.69	0.63	0.70	
75th d_I		0.58	0.64	0.56	0.66	
Average d_I		0.62	0.68	0.61	0.69	
25th WBE		35	29	53	25	
Median WBE		22	20	33	18	
75th WBE		15	12	18	11	
Average WBE		27	23	36	19	

Comments

Second, please check upon equation 20, as now, indeed, the formula does not refer to the absolute water balance error (MAE) but to the relative mean absolute error: or equation 20 is adjusted appropriately, or, the MAE is used throughout the remainder of the text.

Response:

We have corrected Equation (20) for the water balance error (WBE). The revision has been made. We also update our paper such as descriptions of results and figures according to this change.

--Line 352.

$$WBE = \frac{\sum_{i=1}^N |Q_{sim,i} - Q_{obs,i}|}{\sum_{i=1}^N Q_{obs,i}} \times 100\% \quad (19)$$

--Line 943-946.

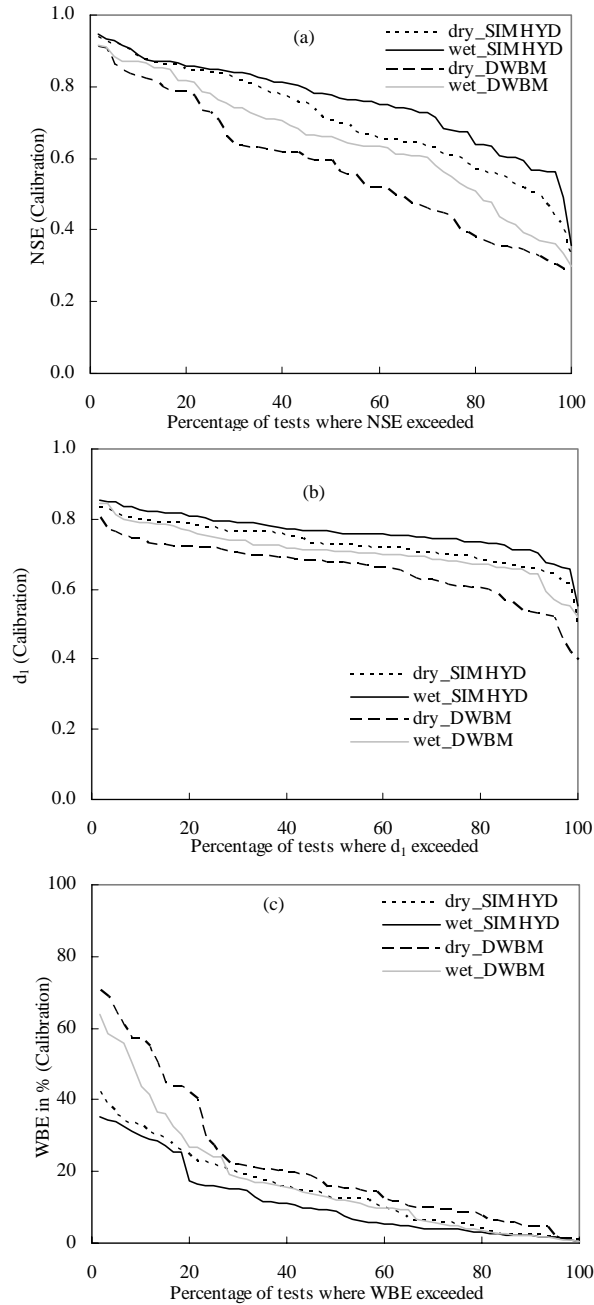
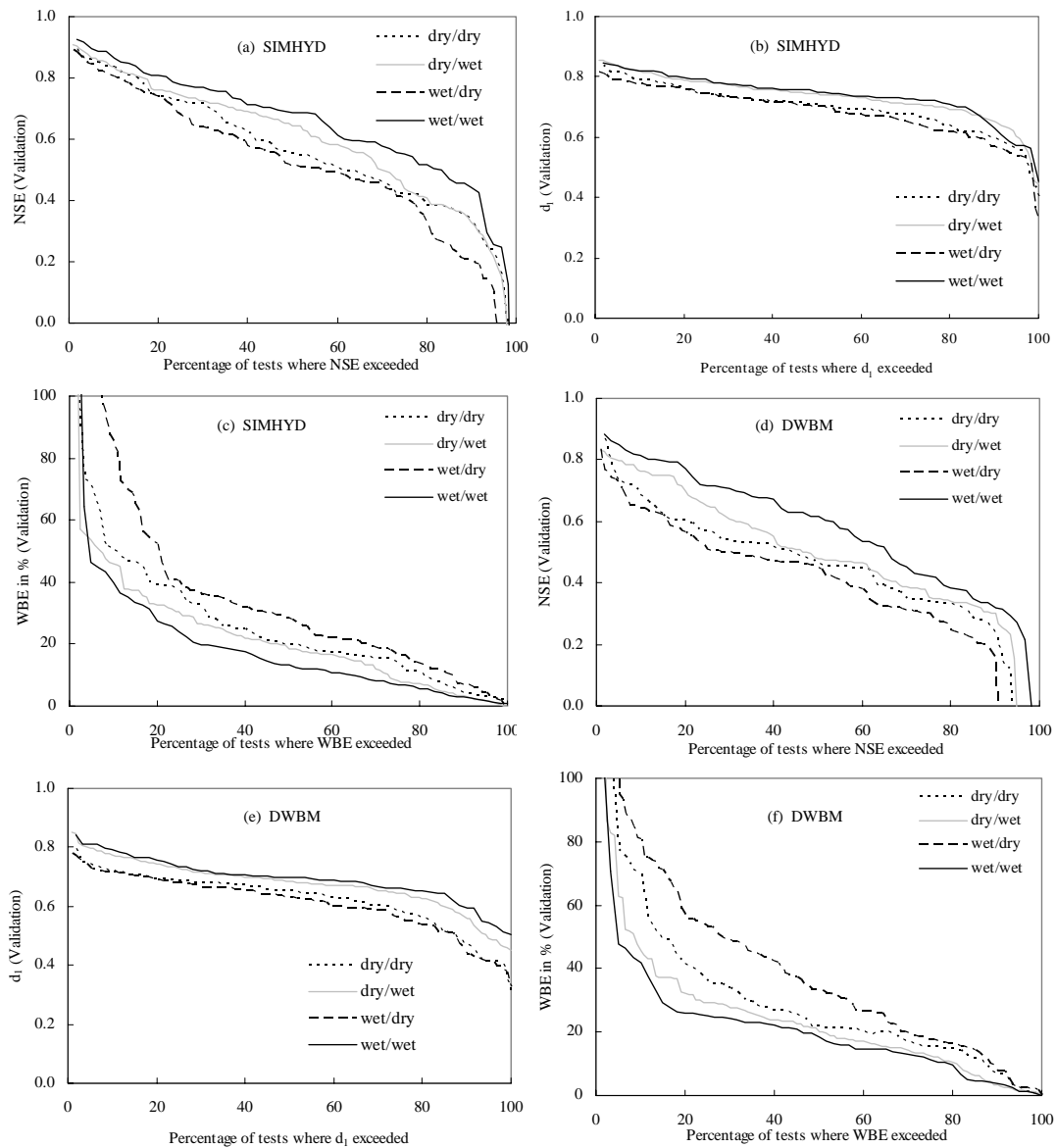


Figure 5 (a) Percentage of model calibration tests with a NSE value greater than or equal to a given NSE value. Similarly, **Figure 5 (b-c)** are corresponding plots of the modified index of agreement (d_1) and the water balance error (WBE), respectively.

--Line 947-953.



Figures 6 (a) and (d) Percentage of model validation tests with a NSE value greater than or equal to a given NSE value. Similarly, **Figures 6 (b) and (e)**, **Figures 6 (c) and (f)** are corresponding plots of the modified index of agreement (d_1), the water balance error (WBE), respectively.

1 **The transferability of hydrological models under nonstationary**
2 **climatic conditions**

3

4 Chuanzhe Li^{1,2,3}, Lu Zhang^{2,*}, Hao Wang¹, Yongqiang Zhang², Fuliang Yu¹ and
5 Denghua Yan¹

6

7 ¹ State Key Laboratory of Simulation and Regulation of Water Cycle in River Basin,
8 China Institute of Water Resources and Hydropower Research, Beijing 100038, P.R.
9 China

10 ² CSIRO Land and Water, Canberra ACT 2601, Australia

11 ³ State Key Laboratory of Hydrology-Water Resources and Hydraulic Engineering,
12 Hohai University, Nanjing 210098, P.R. China

13

14 * Corresponding author: Lu Zhang, CSIRO Land and Water, GPO Box 1666,
15 Canberra ACT 2601, Australia

16 Tel: +61(2)6246-5802

17 Fax: +61(2)6246-5800

18 Email: lu.zhang@csiro.au

19

20 Submission to: Hydrology and Earth System Sciences

21

22 Submission date: September, 2011

23

24 **Abstract:** This paper investigates issues involved in calibrating hydrological models
25 against observed data when the aim of the modelling is to predict future runoff under
26 different climatic conditions. To achieve this objective, we tested two hydrological
27 models, DWBM and SIMHYD, using data from 30 unimpaired catchments in
28 Australia which had at least 60 years of daily precipitation, potential
29 evapotranspiration (PET), and streamflow data. Nash–Sutcliffe efficiency (NSE),
30 modified index of agreement (d_1) and water balance error (WBE) were used as
31 performance criteria. We used a differential split-sample test to split up the data into
32 120 sub-periods and 4 different climatic sub-periods in order to assess how well the
33 calibrated model could be transferred different periods. For each catchment, the
34 models were calibrated for one sub-period and validated on the other three. Monte
35 Carlo simulation was used to explore parameter stability compared to historic climatic
36 variability. The chi-square test was used to measure the relationship between the
37 distribution of the parameters and hydroclimatic variability. The results showed that
38 the performance of the two hydrological models differed and depended on the model
39 calibration. We found that if a hydrological model is set up to simulate runoff for a
40 wet climate scenario then it should be calibrated on a wet segment of the historic
41 record, and similarly a dry segment should be used for a dry climate scenario. The
42 Monte Carlo simulation provides an effective and pragmatic approach to explore
43 uncertainty and equifinality in hydrological model parameters. Some parameters of
44 the hydrological models are shown to be significantly more sensitive to the choice of
45 calibration periods. Our findings support the idea that when using conceptual
46 hydrological models to assess future climate change impacts, a differential
47 split-sample test and Monte Carlo simulation should be used to quantify uncertainties
48 due to parameter instability and non-uniqueness.

49

50 **KEY WORDS:** Hydrological models; nonstationarity; calibration; validation; climate
51 change

52

53 **1 Introduction**

54 Climate change caused by increasing atmospheric concentration of greenhouse gases
55 may have significant effects on the hydrological cycle and water availability, hence
56 affecting agriculture, forestry, and other industries (*Rind et al.*, 1992; *IPCC*, 2007).

57 Changes in the hydrological cycle may mean more floods and droughts, and increased
58 pressure on water supply and irrigation systems. It is important for us to be able to
59 estimate the potential impact of climate change on water resources and develop
60 sustainable management strategies. One of the challenges in predicting hydrological
61 response to climate change is the issue of hydrological nonstationarity (*Milly et al.*,
62 2008). There are numerous factors that can affect hydrological stationarity and these
63 include vegetation responses to elevated CO₂, changes in land use and rainfall
64 characteristics. It is crucial to improve our understanding of the effect of
65 nonstationarity on hydrological assessments of climate change.

66

67 Hydrological models are important tools for predicting the impact of climate change
68 on future water resources and associated socioeconomic impacts. A number of models
69 have been used to evaluate hydrological effects of climate change (*Rind et al.*, 1992).

70 Predicting the hydrological impacts of climate change involves two key steps:

71 downscaling the outputs from global climate models (GCMs) and then running

72 hydrological models. At present, outputs from different GCMs have been used to

73 drive hydrological models for predicting streamflow under a changed climate (Chiew
74 *et al.*, 2009). There are many factors that can affect the accuracy of a rainfall-runoff
75 model in predicting the hydrological responses to climate change, including the
76 particular hydrological model chosen, the GCM used, the optimisation technique
77 employed, and the calibration period of the model. Most researchers usually use an
78 ensemble of these techniques to minimise the uncertainty in predicting climate change
79 impacts. For instance, *Chiew et al.* (1995) used results from 5 separate GCM
80 experiments and reported that, in certain parts of Australia, the GCMs did not even
81 agree on the direction of change in rainfall (i.e. increasing or decreasing rainfall).
82 *Boorman and Sefton.* (1997) evaluated effects of climate change on mean runoff,
83 flood magnitude, and low flow for 3 catchments in UK using 2 conceptual
84 rainfall-runoff models. In their study, they considered 2 climate scenarios and 8
85 climate sensitivity tests. *Minville et al.* (2008) produced an uncertainty envelope of
86 future hydrological variables by considering 10 equally weighted climate projections
87 from a combination of 5 GCMs and 2 greenhouse gas emission scenarios. *Monomoy*
88 *and O'Connor* (2007) used 6 automatic optimisation techniques to calibrate a
89 conceptual rainfall-runoff model, and there have been a number of more recent
90 studies for estimating the impact of climate change on hydrological processes (*Chiew*
91 *et al.*, 2009, *Vaze et al.*, 2010, *Boyer et al.*, 2010). An implicit assumption in all these
92 studies is that rainfall-runoff models calibrated over the historical period are valid for
93 predicting the future hydrological regime under a changed climate and this relates
94 directly to the assumption of hydrological stationarity. However, little has been
95 carried out to test the validity of this assumption.
96

97 Calibration of hydrological models generally involves optimizing model parameters to
98 match measured streamflow using observed rainfall as input. Performance of the
99 model is usually tested using a simple split-sample test, i.e. the model is calibrated for
100 one period of the record and tested for another period. The simple split-sample test
101 may be sufficient for applications where hydroclimatic conditions between the
102 calibration period and validation period are similar. However, when the model needs
103 to be applied to simulate streamflow from periods with different conditions from
104 those in the calibration periods, a more powerful test is required (*Klemes*, 1986, *Xu*,
105 1999, *Seibert*, 2003). In a recent paper, *Andreassian et al* (2009) used crash test to
106 advocate for more comprehensive model testing in hydrology. For predicting the
107 impact of climate change on streamflow, the input rainfall series are varied according
108 to an assumed future climate scenario and this often means different climatic
109 conditions. But is it appropriate to use these models for future climatic conditions
110 when rainfall–runoff relations could be very different to those experienced
111 historically?

112

113 This paper investigates the transferability of hydrological models under nonstationary
114 climatic conditions. We compare results obtained with different hydrological models
115 calibrated under different climatic conditions. The paper first presents two
116 hydrological models chosen for this study – the Dynamic Water Balance Model
117 (DWBM) and the SIMHYD model – and then describes the data used to calibrate
118 them. We describe different methods of applying the data, including a differential
119 split-sample test, a Monte Carlo simulation, and a performance criterion. Finally, we
120 analyse the performance of the models under different calibration conditions and
121 discuss the optimal parameters for each.

122

123 **2 Description of Hydrological Models and Data**

124 Two lumped hydrological models with daily inputs were chosen for this study: the
125 Dynamic Water Balance Model (DWBM) (*Zhang et al.*, 2008) and the SIMHYD
126 model (*Chiew et al.*, 2002), and detailed description of the two models is presented
127 below.

128

129 **2.1 The Dynamic Water Balance Model (DWBM)**

130 The DWBM model used in this study was developed by *Zhang et al.* (2008). It is a
131 lumped conceptual water balance model with two stores: a near surface root-zone
132 store and a deeper zone store (**Figure 1**). The model is based on Budyko's concept of
133 water availability and atmospheric demand (Budyko, 1958) or the concept of "*limits*
134 *and controls*" (*Calder*, 1998). Fundamental to this model is a functional form that
135 represents a smooth transition between supply and demand limits (*Fu*, 1981):

$$136 \quad \frac{E}{P} = 1 + \frac{E_0}{P} - \left[1 + \left(\frac{E_0}{P} \right)^w \right]^{1/w} \quad (1)$$

137 where w is a model parameter ranging between 1 and ∞ . For the purpose of model
138 calibration, we define $\alpha = 1 - 1/w$ so that α varies between 0 and 1. This definition also
139 conveniently associates an increase in α with an increase in evapotranspiration
140 efficiency. P is rainfall and E_0 is potential evapotranspiration at mean annual
141 timescale. More details of this mean annual water balance model are given in *Zhang*
142 *et al.* (2004) and *Zhang et al.* (2008).

143 It is assumed that rainfall $P(t)$ in time step t will be partitioned into direct runoff $Q_d(t)$
144 and catchment rainfall retention:

145
$$P(t) = Q_d(t) + X(t) \tag{2}$$

146 where $X(t)$ is called catchment rainfall retention and is the amount of rainfall retained
 147 by the catchment for evapotranspiration $ET(t)$, change in soil moisture storage
 148 $S(t)-S(t-1)$ and recharge $R(t)$.

149 The demand limit for $X(t)$ is the sum of available storage capacity ($S_{max}-S(t-1)$) and
 150 potential evapotranspiration ($E_0(t)$) and is denoted as $X_0(t)$, while the supply limit can
 151 be considered as rainfall $P(t)$. Following a similar argument to *Budyko* (1958), we can
 152 postulate that:

153
$$X(t)/P(t) \rightarrow 1 \quad \text{as} \quad X_0(t)/P(t) \rightarrow \infty \quad (\text{very dry conditions}) \tag{3}$$

154
$$X(t) \rightarrow X_0(t) \quad \text{as} \quad X_0(t)/P(t) \rightarrow 0 \quad (\text{very wet conditions}) \tag{4}$$

155 The catchment rainfall retention $X(t)$ can be calculated as:

156
$$X(t) = P(t)F\left(\frac{X_0(t)}{P(t)}, \alpha_1\right) \tag{5}$$

157 where $F(\)$ is Fu's curve – equation (1), α_1 is rainfall retention efficiency, i.e., a larger
 158 α_1 value will result in more rainfall retention and less direct runoff.

159 From equations (2) and (5), direct runoff is calculated as:

160
$$Q_d(t) = P(t) - X(t) \tag{6}$$

161 At sub-annual time scales, water availability $W(t)$ can be defined as:

162
$$W(t) = X(t) + S(t-1) \tag{7}$$

163 Combining the definition of $X(t)$ with equation (7), one obtains:

164
$$W(t) = ET(t) + S(t) + R(t) \tag{8}$$

165 While equation (7) defines the source of the water availability, Equation (8)
 166 determines the partitioning. Next define evapotranspiration opportunity
 167 (*Sankarasubramanian and Vogel, 2002*) as $Y(t) = ET(t) + S(t)$, we obtain:

168
$$W(t) = Y(t) + R(t) \tag{9}$$

169 The demand limit for $Y(t)$ can be considered as the sum of potential
 170 evapotranspiration ($E_0(t)$) and soil water storage capacity (S_{max}) and is denoted as $Y_0(t)$,
 171 while the supply limit is the available water $W(t)$. Similar to *Budyko* (1958), we can
 172 postulate that:

$$173 \quad Y(t)/W(t) \rightarrow 1 \quad \text{as} \quad Y_0(t)/W(t) \rightarrow \infty \quad (\text{very dry conditions}) \quad (10)$$

$$174 \quad Y(t) \rightarrow Y_0(t) \quad \text{as} \quad Y_0(t)/W(t) \rightarrow 0 \quad (\text{very wet conditions}) \quad (11)$$

175 The evapotranspiration opportunity $Y(t)$ can be estimated from the following
 176 relationship:

$$177 \quad Y(t) = W(t)F\left(\frac{E_0(t)+S_{max}}{W(t)}, \alpha_2\right) \quad (12)$$

178 Thus groundwater recharge $R(t)$ can be calculated from Equation (9). The next step is
 179 to calculate evapotranspiration $ET(t)$. The demand limit for $ET(t)$ can be considered as
 180 potential evapotranspiration $E_0(t)$ and the supply limit is the available water $W(t)$.
 181 Similar to *Budyko* (1958), evapotranspiration $ET(t)$ can be calculated as:

$$182 \quad ET(t) = W(t)F\left(\frac{E_0(t)}{W(t)}, \alpha_2\right) \quad (13)$$

183 where α_2 is a model parameter, representing evapotranspiration efficiency.

184 Soil water storage can now be calculated as:

$$185 \quad S(t) = Y(t) - ET(t) \quad (14)$$

186 Finally, groundwater storage is treated as linear reservoir, so that baseflow and
 187 groundwater balance can be modelled as:

$$188 \quad Q_b(t) = dG(t-1) \quad (15)$$

$$189 \quad G(t) = (1-d)G(t-1) + R(t) \quad (16)$$

190 where Q_b is baseflow, G is groundwater storage, and d is a recession constant.

191

192 The DWBM model has been applied to 265 catchments in Australia and showed
193 encouraging results (*Zhang et al.*, 2008). The model has four parameters: retention
194 efficiency(α_1); evapotranspiration efficiency(α_2); soil water storage capacity (S_{max}),
195 and baseflow linear recession constant (d). The range of the parameter values is
196 shown in **Table 1**.

197

198 **[Figure 1 and Table 1 here]**

199

200 **2.2 The SIMHYD Model**

201 The SIMHYD model is a lumped conceptual daily rainfall–runoff model (*Chiew et al.*,
202 2002), driven by daily rainfall and PET, which simulates daily streamflow. It has been
203 tested and used extensively across Australia (*Chiew et al.*, 2002; *Siriwardena et al.*,
204 2006; *Viney et al.*, 2008; *Zhang et al.*, 2008; *Zhang et al.*, 2009). **Figure 2** shows the
205 structure of the SIMHYD model and the algorithms controlling how water enters the
206 system from precipitation, flows into several stores, and then flows out through
207 evapotranspiration and runoff. The SIMHYD model has 7 parameters, and the useful
208 ranges of them are shown in **Table 2**.

209

210 **[Figure 2 and Table 2 about here]**

211

212 In the SIMHYD model, daily rainfall is first intercepted by an interception store,
213 which is emptied each day by evaporation. Incident rainfall, which occurs if rainfall
214 exceeds the maximum daily interception, is then subjected to an infiltration function.
215 The incident rainfall that exceeds the infiltration capacity becomes infiltration excess
216 runoff. A soil moisture function diverts the infiltrated water to the river (as saturation

217 excess runoff/interflow), groundwater store (as recharge) and soil moisture store. The
218 saturation excess runoff/interflow is first estimated as a linear function of the soil
219 wetness (soil moisture level divided by soil moisture capacity). The equation used to
220 simulate interflow therefore attempts to mimic both the interflow and saturation
221 excess runoff processes (with soil wetness used to reflect those parts of the catchment
222 that are saturated and from which saturation excess runoff can occur). Groundwater
223 recharge is then estimated, also as a linear function of the soil wetness. The remaining
224 moisture flows into the soil moisture store. Evapotranspiration from the soil moisture
225 store is estimated as a linear function of the soil wetness, but cannot exceed the
226 potential rate (PET minus intercepted water). The soil moisture store has a finite
227 capacity and overflows into the groundwater store, baseflow from which is simulated
228 as a linear recession from the groundwater store. The model has therefore three runoff
229 components: infiltration excess runoff, saturation excess runoff/interflow, and
230 baseflow.

231

232 **2.3 Study Catchments and Data**

233 In this study 30 catchments from Australia were selected with at least 60 years of
234 unimpaired daily streamflow data (**Figure 3**). Unimpaired streamflow is defined as
235 streamflow that is not subject to regulation or diversion. The catchment area ranges
236 from 82 to 1891 km² with mean annual streamflow varied between 53 to 1363 mm.
237 The mean annual precipitation (*P*) ranges from 628 to 2095 mm and annual potential
238 evapotranspiration (*PET*) ranges from 817 to 2098 mm, representing diverse
239 hydrological and climatic conditions. The runoff coefficient varies from 0.08 to 0.65.
240

241 Catchment averaged annual rainfall was estimated from gridded SILO daily rainfall
242 (<http://www.longpaddock.qld.gov.au/silo>, Jeffrey *et al.*, 2001). The SILO Data Drill
243 provides surfaces of daily rainfall and other climate data interpolated from point
244 measurements made by the Australian Bureau of Meteorology. The spatial resolution
245 of the gridded daily rainfall data is 0.05 degrees based on interpolation of over 6000
246 rainfall stations across Australia. The interpolation uses monthly rainfall data,
247 ordinary kriging with zero nugget, and a variable range. Monthly rainfall for each $5 \times$
248 5 km grid cell was converted to daily rainfall using daily rainfall distribution from the
249 station closest to the grid cell (Jeffrey *et al.*, 2001). The daily time series of maximum
250 and minimum temperatures, incoming solar radiation, actual vapour pressure, and
251 precipitation at 0.05×0.05 (~ 5 km \times 5 km) grid cells from the SILO Data Drill
252 (<http://www.longpaddock.qld.gov.au/silo>) were used.

253

254 Potential evaporation was calculated using the Priestley-Taylor equation (Priestley
255 and Taylor, 1972) for each catchment with the Priestley-Taylor coefficient set to 1.26
256 following Raupach (2000). In the calculation, the available energy was taken as equal
257 to the net radiation by neglecting ground heat flux. The net radiation was calculated
258 from the incoming global shortwave and longwave radiation, surface albedo, surface
259 emissivity, and surface temperature as described by Raupach *et al.* (2001).

260

261 Daily streamflow data were obtained from the Australian Land and Water Resources
262 Audit project (Peel *et al.*, 2000) and have been quality checked. Firstly, data quality
263 codes were checked for any missing and poor-quality data as most gauging stations
264 provide numerical codes indicating quality of streamflow data. Missing streamflow
265 data were infilled by interpolating streamflow values at previous and following days.

266 Secondly, time series of daily rainfall and streamflow were plotted to identify any
267 inconsistency and recording errors in the data (e.g. spikes, same streamflow value for
268 a long period of time). The quality checks are to ensure good quality streamflow data
269 are used in the study.

270

271

[Figure 3 here]

272

273 **3 Methods**

274 **3.1 Differential Split-sample Test**

275 In general, hydrological models rely on stationary conditions (*Xu, 1999*). Usually,
276 model calibration requires a split-sample test, where the model is calibrated during
277 one climatic period and validated on another independent period. The split-sample test
278 is the classical test, being applicable to cases where there is sufficiently long time
279 series of the climatic data for both calibration and validation and where the catchment
280 conditions remain unchanged, i.e. stationary (*Refsgaard and Storm, 1996*). This test
281 gives an indication how the model might perform for an independent period having
282 similar conditions. Unfortunately, this test is unable to guarantee the applicability of
283 hydrological models under nonstationary conditions (*Xu, 1999; Henriksen et al.,*
284 *2003*).

285

286 In order to try to answer the question of whether the transfer of parameter values from
287 the present-day climate to a future climate is justified, the ‘differential split-sample
288 test’ proposed by *Klemes (1986)* was considered, in which the hydrological model is

289 tested on calibration and validation periods under contrasting climatic conditions. In
290 this case, different sub-periods are chosen with different historical rainfall conditions.

291

292 In this study, different periods with various climatic conditions were identified. First
293 of all, we calculated annual and mean annual precipitation over the whole period of
294 record for each catchment. Then sub-periods with consecutive annual precipitation
295 greater than the mean were selected as the “wet” periods and sub-periods with
296 consecutive annual precipitation less than the mean were selected as the “dry” periods.
297 The precipitation in the “wet” periods is 10.2% to 47.1% above the long-term average
298 annual precipitation, while the precipitation in the “dry” periods is 10.4% to 28.3%
299 below the long-term average annual precipitation. In the selection, the minimum
300 length of the sub-period was set to 5 years to ensure stable model calibration. If this
301 process results in more than two “wet” or “dry” periods, then the two wettest periods
302 or two driest periods were selected for model calibration and validation (**Figure 4**).
303 The hydrological model was calibrated for each of the 4 sub-periods and validated on
304 each of the remaining 3 sub-periods in turn, resulting in a total of 12 calibration and
305 validation tests.

306

307 To examine model performance under different calibration and validation conditions,
308 results from the above tests are grouped as “**dry**/dry”, “**dry**/wet”, “**wet**/wet”, and
309 “**wet**/dry” to represent climatic conditions in the calibration and validation periods
310 respectively.

311

312

[Figure 4 about here]

313

314 3.2 Monte Carlo Simulation

315 It has been widely recognized that hydrological models can perform equally well
316 against measured runoff estimates even with different parameter sets and this
317 so-called parameter equifinality may result in large prediction uncertainty (*Beven,*
318 *1993; Boorman et al., 1997; Niel et al., 2003; Wilby et al., 2005; Minville et al., 2008*).
319 The parameter equifinality is related to overparameterization of hydrological models
320 and poor parameter identifiability. For some practical applications, the parameter
321 equifinality problem may not be an issue and any of the parameter sets may be
322 appropriate. However, these equally good parameter sets may give different
323 predictions when the model is used to estimate the effects of climate change and land
324 use change on streamflow (*Uhlenbrook et al., 1999*). The need for improved model
325 calibration and testing has been emphasized in recent years. Monte Carlo simulation is
326 an effective way of calculating confidence limits of predicted time series and
327 exploring parameter stability and identifiability in the context of historic climate
328 variability (*Uhlenbrook et al., 1999; Wilby, 2005; Widen-Nilsson et al., 2009*).

329

330 For each catchment and each calibration period, a Monte Carlo simulation was
331 undertaken with 1,000,000 runs, each with randomly generated parameter values
332 within the given ranges listed in **Tables 1** and **2** for the two models respectively. We
333 then selected assemblies of the 100 best parameter sets for each catchment and each
334 calibration period according to a goodness-of-fit measure which is defined in section
335 3.3. Finally, the models were run during the validation periods with all the 100 best
336 parameter sets. Calibration with the 100 best parameter sets gave very similar results
337 and the means were used in subsequent analysis.

338

339 3.3 Model Performance Criteria

340 The Nash–Sutcliffe efficiency (NSE) (*Nash and Sutcliffe, 1970*) was used as the
341 statistic criterion of the model performance. The objective function used in the model
342 calibration is the Nash and Sutcliffe efficiency of daily runoff, which is defined as:

$$343 \quad NSE = 1 - \frac{\sum_{i=1}^N (Q_{obs,i} - Q_{sim,i})^2}{\sum_{i=1}^N (Q_{obs,i} - \overline{Q_{obs,i}})^2} \quad (17)$$

344 where $Q_{sim,i}$ and $Q_{obs,i}$ are the simulated and observed daily runoff, respectively,
345 $\overline{Q_{obs,i}}$ is the mean observed runoff, i is the i th day, and N is the number of days
346 sampled and it varies with individual catchment.

347

348 Following recommendations by Legates and McCabe (1999) and Hogue et al., 2006,
349 two statistics are used to indicate the accuracy of the SIMHYD and DWBM models:
350 the modified index of agreement (d_1) and the water balance error (WBE):

$$351 \quad d_1 = 1.0 - \frac{\sum_{i=1}^N |O_{obs,i} - O_{sim,i}|}{\sum_{i=1}^N (|O_{sim,i} - \overline{O_{obs,i}}| + |O_{obs,i} - \overline{O_{obs,i}}|)} \quad (18)$$

$$352 \quad WBE = \frac{\sum_{i=1}^N |Q_{sim,i} - Q_{obs,i}|}{\sum_{i=1}^N Q_{obs,i}} \times 100\% \quad (19)$$

353 with the symbols defined above.

354

355 3.4 Analysis of Parameter Probability Distributions under Different Calibration 356 Periods

357 For each of the models, we ended up with 100 best parameter sets for each catchment
358 and for each calibration period. From these parameters sets we calculated a
359 probability distribution of each parameter. For a given significance level α , the
360 chi-square test (χ^2 test) was used to test the null hypothesis that the parameter
361 distributions obtained for a dry period and a wet period were significantly different. A
362 p value greater than 0.01 indicates a rejection of the null hypothesis, which means that
363 the parameter probability distributions for the two different calibration periods are
364 similar.

365

366 **4 Results**

367 **4.1 Comparisons of Model Calibration under Different Climatic Conditions**

368 Results of model calibration under different climatic conditions are shown in **Figure 5**
369 and **Table 3**. **Figure 5(a)** shows the percentage of model calibration tests that have a
370 NSE value exceeding a given NSE value. Similarly, **Figure 5(b-c)** are corresponding
371 plots of the modified index of agreement (d_1), the water balance error (WBE),
372 respectively. It can be seen that the SIMHYD model was well calibrated under both
373 dry and wet conditions. The average value is greater than 0.70 for NSE, 0.73 for d_1 .
374 The average water balance error is 14% and 11% for the dry and wet calibration
375 periods. Compared with the SIMHYD model, the DWBM model showed slightly
376 poorer results. The average value for the DWBM model is greater than 0.57 for NSE,
377 0.65 for d_1 . The average water balance error is 22% and 17% for the dry and wet
378 calibration periods.

379

380 The plots show that both models were better calibrated under wet periods than under
381 dry ones, with higher values of NSE and d_1 and lower values of WBE in the wet
382 calibration periods. For example, under the dry conditions, average NSE was 0.70 and
383 0.57 for the SIMHYD and the DWBM model. Under the wet conditions, average NSE
384 was 0.76 and 0.65 respectively for the two models. In **Figure 5(a)**, a larger NSE value
385 means a better performance, whereas in **Figure 5(c)**, a smaller percentage WBE value
386 is better. It can be noted that all the results became worse when the calibration periods
387 became drier, indicating a higher sensitivity of the models to dry climatic conditions.
388 The results also indicated that the errors in the simulated runoff were increased under
389 drier climatic conditions.

390

391 It can be seen from Table 3 that under dry and wet calibration periods, the median
392 NSE values are, for the SIMHYD model, 0.70 and 0.77, respectively, and for the
393 DWBM model, 0.58 and 0.66. The median d_1 values showed similar patterns under
394 dry and wet calibration conditions. The median percentile of the WBE values are 13%
395 and 8% for the SIMHYD model under dry and wet calibration periods respectively,
396 and 15% and 12% for the DWBM model. All these results indicate that the two
397 models can be calibrated satisfactorily for most of the tests, although the calibration
398 results of the DWBM model are slightly poorer compared with those of the SIMHYD
399 model. The average NSE values calibrated under the wet periods are higher – i.e.
400 better – by 0.06 (SIMHYD model) and 0.08 (DWBM model) than those calibrated
401 under dry periods. The average WBE values calibrated under wet periods are lower –
402 again better – by 3% (SIMHYD model) and 5% (DWBM model) than those calibrated
403 under the dry period.

404

405 [Figure 5 and Table 3 about here]

406

407 4.2 Comparisons of Model Validation using Different Calibration Periods

408 Validation runs were conducted for 60, 120, 60, and 120 tests for the **dry/dry**, **dry/wet**,
409 **wet/dry**, and **wet/wet** groups, respectively. The model validation results are
410 summarized in **Figure 6 and Table 4**. As expected, the validation results are slightly
411 poorer than the calibration results, with the averaged NSE values in the model
412 validation generally being 0.1 to 0.2 lower than those in the model calibration and
413 percentage water balance error being 2 to 7% higher.

414

415 Comparing the validation results of the **dry/dry**, **dry/wet**, **wet/dry**, and **wet/wet**
416 groups in **Figure 6**, it can be noted both the SIMHYD and DWBM models gave
417 similar patterns. The results for the **wet/wet** are better than those of the **dry/wet** – this
418 means that the models performed better during a wet period when they are calibrated
419 against a wet period, compared to when they are calibrated against a dry period. These
420 results suggest, not unexpectedly, that if a hydrological model is intended to simulate
421 streamflow for a wet climate period then it should be calibrated on a wet segment of
422 the historic record. They also show that hydrological models will, in general, perform
423 better when calibrated in a wet period than when calibrated in the dry period.

424

425 **Table 4** summarizes the 25th percentile, median, 75th percentile, and average values of
426 NSE, d_1 and WBE in the validation periods. The results from the **dry/dry** test are
427 slightly better than the results from the **wet/dry** test in terms of NSE, d_1 and WBE.
428 The results indicate, again reasonably, that the hydrological models perform better in
429 a dry period when calibrated in a dry period rather than in a wet period.

430

431

[Figure 6 and Table 4 about here]

432

433 **4.3 Parameter Uncertainty under Climatic Nonstationarity**

434 As described in section 3.2, assemblies of the 100 best parameter sets were selected
435 from Monte Carlo simulation under different calibration conditions. **Table 5** shows
436 the percentage of the catchments in which the model parameter distributions for a dry
437 and wet period were significantly different ($p < 0.01$). For each model, the parameters
438 are ranked from the most sensitive to calibration conditions to least sensitive. For the
439 SIMHYD model, the most sensitive parameters were SUB, SMSC, SQ, and CRAK,
440 each of which significantly affected 50% or more of the catchments. The other three
441 parameters, K, COEFF, and INSC had smaller effects, with INSC (having an effect in
442 only 10% of catchments) being the most insensitive to choice of dry and wet
443 calibration periods.

444

445

[Table 5 about here]

446

447 In order to further examine the effects of climatic conditions on the results, we
448 grouped the 30 study catchments into two climatic types: 16 water-limited catchments
449 with an index of dryness (E_p/P) greater than 1, and 14 energy-limited catchments with
450 an index of dryness less than 1. It can be noted that all parameters performed
451 differently in water-limited and energy-limited catchments, in particular SUB, SMSC,
452 and CRAK.

453

454 For the DWBM model, the parameters α_1 and S_{max} exhibited different effects on
455 runoff under the dry and wet calibration periods as 67% and 63% of the catchments
456 showed statistically different results at the 0.01 level. At the other extreme, the
457 parameter α_2 displayed an apparent insensitivity to the calibration periods (just 23%
458 of catchments were affected). The parameter α_2 represents evapotranspiration
459 efficiency and it behaves similarly to the parameter w of *Zhang et al.* (2001) and
460 (2004), which was shown to be mostly correlated with vegetation cover. The
461 parameter d was more sensitive to the choice of the calibration period for the
462 water-limited catchments than for the energy-limited catchments. It is interesting to
463 note that all the parameters behaved differently under the water-limited and
464 energy-limited conditions, except perhaps for parameter α_2 .

465

466 The above results indicate that some of the model parameters are sensitive to
467 calibration conditions and the others are relative robust. An important question is how
468 the sensitive parameters vary between the different calibration periods. **Figures 7** and
469 **8** show the distributions of the optimized parameters of the two models under the dry
470 and wet conditions in two selected catchments. The catchment 110003 has
471 summer-dominant rainfall and catchment 401210 is winter-dominant. For the
472 SIMHYD model, some parameters exhibited different distributions in the dry and wet
473 calibration periods. For example, the parameter SUB tends to be more likely at a
474 higher value in the dry periods than in the wet periods. However, the results did not
475 reveal any systematic trends in the other parameters. For the DWBM model, the most
476 likely value for the parameter α_1 was higher in the dry period than in the wet period
477 for catchment 110003 and vice versa for catchment 401210 (**Figure 8**). The parameter

478 S_{max} showed different distributions in the dry and wet periods and these distributions
479 vary across the catchments.

480

481 **[Figures 7 and 8 about here]**

482

483 **5 Discussion**

484 Streamflow of a catchment is influenced by a number of factors, most noticeably
485 rainfall and antecedent soil moisture. During dry periods, catchments are generally
486 characterized by small runoff events and lower runoff to rainfall ratios with higher
487 percentage error in both rainfall and runoff. In this case, rainfall-runoff models
488 become very sensitive to both rainfall and parameter optimization. Also, dry periods
489 may not contain enough high flows to adequately calibrate model parameters
490 responsible for simulating high flows (*Gan et al.*, 1997). Apart from rainfall amount,
491 spatial variability of rainfall can also affect runoff. *Smith et al.* (2004) showed that
492 improved runoff simulations can be obtained from distributed versus lumped
493 rainfall-runoff models in catchments with considerable rainfall variability. Spatial
494 variability of rainfall was also found to be the dominant control on runoff production
495 (*Segond et al.*, 2007). In this study, spatially averaged rainfall was used in both model
496 calibration and validation. This is likely to affect the model results and it is expected
497 that the rainfall variability effect will be greater in dry periods than in wet periods.

498

499 It has been widely acknowledged that spatial variability of antecedent soil moisture
500 conditions plays an important role in runoff generation (*Grayson and Blöschl*, 2000).
501 *Minet et al.* (2011) investigated the effect of spatial soil moisture variability on runoff
502 simulations using a distributed hydrologic model and showed that model results are

503 sensitive to soil moisture spatial variability, especially in dry conditions. At catchment
504 scales, soil moisture exhibit larger heterogeneity under dry conditions than wet
505 conditions and this means errors associated with dry period runoff simulations are
506 likely to be greater as runoff generation exhibits non-linear threshold behaviour.
507 In this study, the differences in average annual rainfall between the wet and dry
508 periods ranged from 10 to 47% of the long-term average rainfall and are comparable
509 with percentage change in mean annual rainfall for 2030 relative to 1990 from 15
510 GCMs for the Murray Darling Basin in Australia (*Chiew et al., 2008*).

511

512 The results of this study indicate that calibration periods can cause significant shifts in
513 model parameter distributions. Some model parameters are relatively sensitive to the
514 choice of calibration periods, while the others are fairly insensitive. As well as the
515 impact of calibration periods on parameter distributions, whether catchments are
516 water-limited or energy-limited also needs to be taken into consideration. For the
517 SIMHYD model, the most sensitive parameters are SUB, SMSC, and CRAK. The
518 parameter SUB is used to estimate interflow and it can be an important parameter in
519 some catchments (*Chiew and McMahon, 1994*). However, it is difficult to estimate
520 this parameter *a priori* as it is poorly correlated with any catchment characteristics
521 (*Chiew and McMahon, 1994*). The soil moisture store capacity (SMSC) affects many
522 processes such as infiltration and evapotranspiration and it is determined by soil
523 properties and vegetation characteristics (e.g. rooting depth). Accurate estimation of
524 this parameter is essential to achieving satisfactory model performance. The
525 parameter CRAK determines groundwater recharge/baseflow and is highly correlated
526 with soil types. For the DWBM model, the most sensitive parameters are α_1 and S_{\max} ,
527 and d , representing catchment rainfall retention efficiency, maximum storage capacity,

528 and the recession constant, respectively (*Zhang et al. 2008*). In a way, these
529 parameters are similar to those sensitive parameters in SIMHYD in terms of their
530 functional controls on water balance components. *Merz et al (2011)* applied a
531 semi-distributed conceptual rainfall-runoff model to 273 catchments in Austria and
532 showed that the parameters of the soil moisture accounting schemes exhibited strong
533 dependence on calibration conditions, consistent with the results of the current study.
534 This also suggests that parameters related to soil moisture accounting are likely to
535 change with calibration conditions. The fact that these parameters are sensitive to the
536 choice of calibration period (i.e. dry vs wet) also indicates that large uncertainty may
537 be associated with these parameters and cares need to be exercised when transferring
538 the parameters to conditions different from the calibration.

539

540 These findings have major implications for studies of climate change impact on
541 streamflow. When a hydrological model calibrated for a given climatic condition (e.g.
542 wet periods) is used to simulate runoff of different climatic conditions (e.g. dry
543 periods), transfer of some model parameters (i.e. sensitive parameters) may result in
544 large errors in simulated runoff. One may argue that the sensitive model parameters
545 should be updated by functionally relating them with climatic variables such as
546 rainfall (*Merz et al., 2011*). This could potentially reduce uncertainty and lead to more
547 accurate predictions. However, some of the parameters are poorly related to
548 catchment characteristics (e.g. rainfall) and the problem is further complicated by the
549 fact that not every parameter is well identified and different parameter values can
550 result in equal model performance, i.e. equifinality (*Beven, 1993*). It has also been
551 recognized that model calibration tends to compensate model structural errors (*Merz*

552 et al., 2011, *Wagner et al.*, 2003), making it difficult to understand how model
553 parameters vary with calibration conditions (*Wagener et al.*, 2010).

554

555 The differential split-sample test can be considered as the first step in addressing the
556 issue of parameter transferability under non-stationary conditions. Monte Carlo
557 simulation provided an effective and pragmatic approach to exploring uncertainty in
558 hydrological model parameters. The performance of rainfall-runoff models is related
559 to catchment characteristics such as climate, topography, soil, vegetation, catchment
560 shape, geology, drainage network. In such a complex situation, it is hard to pinpoint
561 the source of parameter uncertainty, but the results of this study showed that
562 calibration periods and catchment climatic conditions are both important factors that
563 can result in uncertainty in model performance.

564

565 Credibility of a hydrological model has traditionally been tested using streamflow
566 data from a validation period that is similar to calibration period. The assumption is
567 that the model will be used under conditions similar to those of the calibration.
568 However, when dealing with impact of climate change on streamflow, the assumption
569 is not generally valid and the model needs to be tested under conditions different from
570 those of the calibration. For this purpose, the two hydrological models were evaluated
571 using differential split-sample test (Klemes, 1986). When using a dry period for
572 calibration and a wet period for validation, the models produced more accurate
573 estimates of streamflow (i.e. higher NSE and lower bias) compared with estimates
574 produced using a wet period for calibration and a dry period for validation (see Table
575 4). Similar results have been reported by Vaze et al. (2010) and the finding can be
576 partly explained by the fact that hydrological models generally perform better in wet

577 periods than in dry periods (Vaze et al., 2010; Gallart et al., 2007, Perrin et al. 2007;
578 Lidén and Harlin, 2000, Gan et al., 1997; Hughes, 1997).

579

580 A closer examination of model errors reveals that when the model parameters,
581 calibrated on a dry period, were used to simulate runoff during a wet period, the mean
582 of the simulated runoff was usually underestimated; conversely, when model
583 parameters, calibrated on a wet period, were used to simulate dry period runoff, the
584 mean simulated runoff was overestimated, consistent with the findings of *Gan et al.*
585 (1997). *Vaze et al.* (2010) also showed that when hydrological models were calibrated
586 using long period of record and tested for sub-periods with above long-term average
587 rainfall, the model performed well. However, performance of the models starts to
588 deteriorate when tested for sub-periods with below long-term average rainfall.

589

590 Traditionally, one would use a sufficiently long period of records for model
591 calibration to ensure proper presentation of climate/streamflow variability and to
592 achieve stable model parameters. If the model is to be used under stationary
593 conditions, it is generally recommended that the whole record should be divided into
594 two segments, one for calibration and the other for validation. However, if a model is
595 to be used under non-stationary conditions, its parameters should be transferable. In
596 other words, the parameters should be estimated so that the model gives accurate
597 estimates of streamflow outside the climatic conditions encountered in calibration
598 period. In this case, one should identify two periods with different climatic
599 conditions (e.g. a dry period and wet period) from the whole record and apply the
600 so-called differential split-sample test (*Klemes*, 1986). One another approach to this

601 problem is to examine how other catchments behave under these different climatic
602 conditions, i.e. trading space for time (*Singh et al.*, 2011).

603

604 **6 Conclusions**

605 Potentially large uncertainties arise when predicting hydrological responses to future
606 climate change – due to factors such as the choice of emission scenario, GCM,
607 downscaling technique, hydrological model, optimization technique, and the way the
608 model is calibrated. It is therefore important to develop reliable ways to calibrate
609 hydrological models under present-day conditions. This study compared hydrological
610 model performances under nonstationarity by using the differential split-sample test
611 and two conceptual rainfall–runoff models, DWBM and SIMHYD, applied to 30
612 catchments in Australia. Monte Carlo simulation was used to explore parameter
613 stability and transferability in the context of historic climate variability.

614

615 Apart from quality of the input data (e.g. rainfall) and model structure, performance of
616 a hydrological model is also dependent on how it is calibrated. If a hydrological
617 model is intended to simulate runoff for a wet climate scenario then it should be
618 calibrated on a wet segment of the historic record. Conversely, if it is intended to
619 simulate runoff for a dry climate scenario then it should be calibrated on a dry
620 segment of the historic record. We also found that when using a dry period for
621 calibration and a wet period for validation, the models produced more accurate
622 estimates of streamflow compared with estimates produced using a wet period for
623 calibration and a dry period for validation. In other words, transferring model
624 parameter values obtained from dry periods to wet periods will result in smaller errors
625 in streamflow estimation than transferring model parameter values obtained from wet

626 periods to dry periods. The soil related model parameters are more sensitive to the
627 choice of calibration period than other parameters and large uncertainty may be
628 introduced when transferring the soil related parameters to conditions different from
629 the calibration. Our research has implications for hydrological modellers looking to
630 estimate future runoff and we hope this study will stimulate further research into the
631 selection of calibration data.

632

633 **Acknowledgement**

634 This study was supported by the National Basic Research Program of China
635 (2010CB951102), the Foundation for Innovative Research Groups of the National
636 Natural Science Foundation of China (51021066), Open Foundation of State Key
637 Laboratory of Hydrology-Water Resources and Hydraulic Engineering (2011490511),
638 the Foundation of China Institute of Water Resources and Hydropower Research
639 (1232) and the Regional Water Theme in the Water for a Healthy Country Flagship.
640 We thank Andrew Bell, Enli Wang and anonymous reviewers for their helpful
641 comments on a draft of the paper.

642 **References**

- 643 Andreassian, V., Perrin, C., Berthet, L., Le Moine, N., Lerat, J., Loumagne, C., Oudin,
644 L., Mathevet, T., Romas, M.-H., Valery, A., 2009. Crash tests for a standardized
645 evaluation of hydrological models. *Hydrol. Earth Syst. Sci.* 13, 1757–1764.
- 646 Beven K J. 1993. Prophecy, reality and uncertainty in distributed hydrological
647 modelling, *Advances in Water Resources*, **16**: 41-51.
- 648 Boorman D B, Sefton C E M. 1997. Recognising the uncertainty in the quantification
649 of the effects of climate change on hydrological response, *Climatic Change*, **35**:
650 415-434.
- 651 Boyer, C, Chaumont, D, Chartier, I, and Roy, A.G. 2010. Impact of climate change on
652 the hydrology of St. Lawrence tributaries, *Journal of Hydrology*, **384**, 65-83.
- 653 Budyko, M.I., 1958. The Heat Balance of the Earth's Surface. US Department of
654 Commerce, Washington, DC.
- 655 Calder, I.R., 1998. Water use by forests, limits and controls, *Tree Physiol*, **18**:
656 625-631.
- 657 Chiew F H S, Whetton P H, McMahon T A, Pittock A B. 1995. Simulation of the
658 impacts of climate change on runoff and soil moisture in Australian catchments,
659 *Journal of Hydrology*, **167**: 121-147.
- 660 Chiew F H S, T A McMahon. 2002. Global ENSO-streamflow teleconnection,
661 streamflow forecasting and interannual variability, *Hydrological Sciences Journal –*
662 *Journal Des Sciences Hydrologiques*, **47**: 505-522.
- 663 Chiew F H S, M C Peel, A W Western. 2002. Application and testing of the simple
664 rainfall–runoff model SIMHYD. In *Mathematical Models of Small Watershed*
665 *Hydrology and Applications*, edited by V. P. Singh and D. K. Frevert, pp. 335-367,
666 Water Resources Publication, Littleton, Colorado, USA.
- 667 Chiew F H S, Teng J, Kirono D, Frost A J, Bathols J M, Vaze J, Viney N R, Young
668 W J, Hennessy K J and Cai W J. 2008. Climate data for hydrologic scenario
669 modelling across the Murray-Darling Basin. A report to the Australian Government
670 from the CSIRO Murray-Darling Basin Sustainable Yields Project. Water for a
671 Healthy Country Flagship. CSIRO. 42 pp.
- 672 Chiew F H S, Teng J, Vaze J, Post D A, Perraud J M, Kirono D G C, Viney N R.
673 2009. Estimating climate change impact on runoff across southeast Australia: method,
674 results, and implications of the modeling method, *Water Resources Research*, **45**:
675 W10414. doi:10.1029/2008WR007338.
- 676 Fu, B P , 1981. On the calculation of the evaporation from land surface, *Sci. Atmos.*
677 *Sin.*, 23-31 (in Chinese).
- 678 Gallart, F., Latron, J., Liorens, P., and Beven, K. 2007. Using internal catchment
679 information to reduce the uncertainty of discharge and baseflow predictions. *Advances*
680 *in Water Resources*, **30**, 808-823.
- 681 Gan T Y, Dlamini E M, Biftu G F. 1997. Effects of model complexity and structure,
682 data quality, and objective functions on hydrologic modelling, *Journal of Hydrology*,
683 **192**: 81-103.

- 684 Grayson, R B and Blöschl G. 2000. Spatial Patterns in Catchment Hydrology:
685 Observations and Modelling. Cambridge University Press. 404pp.
- 686 Henriksen H J, Troldborg L, Nyegaard P, Sonnenborg T O, Refsgaard J C, Madsen B.
687 2003. Methodology for construction, calibration and validation of a national
688 hydrological model for Denmark, *Journal of Hydrology*, **280**: 52-71.
- 689 Hogue S T, Gupta H, Sorooshian S. 2006. A ‘user-friendly’ approach to parameter
690 estimation in hydrologic models, *Journal of Hydrology*, **320**: 202-217.
- 691 Hughes, D.A. 1997. Southern African ‘FRIEND’-the Application of Rainfall-runoff
692 Models in the SADC Region, Report to the Water Research Commission by the
693 Institute for Water Research, Rhodes University, WRC Report No. 235/1/97, Pretoria,
694 South Africa. 69 pp.
- 695 IPCC: Climate Change 2007: The Physical Basis, Contributions of Working Group 1
696 to the Fourth Assessment Report of the Intergovernmental Panel on Climate Change,
697 Solomon, S., Qin, D., Manning, M., Chen, Z., Marquis, M., Averyt, K.B., Tignor, M.
698 and Miller, H.L. (eds.). Cambridge University Press, Cambridge, United Kingdom and
699 New York, USA, 996 pp, 2007.
- 700 Jeffrey S J, Carter J O, Moodie K B, Beswick A R. 2001. Using spatial interpolation
701 to construct a comprehensive archive of Australian climate data, *Environmental*
702 *Modelling & Software*, **16**: 309-330.
- 703 Klemes V. 1986. Operational testing of hydrological simulation models, *Hydrological*
704 *Sciences Journal*, **31**: 13-24.
- 705 Lidén, R. Harlin, J. 2000. Analysis of conceptual rainfall-runoff modeling
706 performance in different climates. *Journal of Hydrology*, **238**, 231-247.
- 707 Merz, R., Parajka, J., and Blöschl, G. 2011. Time stability of catchment model
708 parameters: Implications for climate impact analyses. *Water Resources Research*, 47,
709 W02531, doi:10.1029/2010WR009505.
- 710 Milly P C D, Betancourt J, Falkenmark M, Hirsch R M, Kundzewicz Z W,
711 Lettenmaier D P, Stouffer R J. 2008. Stationarity is dead: whither water management?
712 *Science*, **319**: 573-574.
- 713 Minet J, Laloy E, Lambot S, and Vanclooster M. 2011. Effect of high-resolution
714 spatial soil moisture variability on simulated runoff response using a distributed
715 hydrologic model, *Hydrology and Earth System Sciences*, **15**: 1323-1338.
- 716 Minville M, Brissette F, Leconte R. 2008. Uncertainty of the impact of climate change
717 on the hydrology of a nordic watershed, *Journal of Hydrology*, **358**: 70-83.
- 718 Monomoy G, O’Connor, K.M. 2007. Comparative assessment of six automatic
719 optimization techniques for calibration of a conceptual rainfall-runoff model,
720 *Hydrological Sciences Journal – Journal Des Sciences Hydrologiques*, **52**(3):
721 432-449.
- 722 Nash J E, J V Sutcliffe. 1970. River forecasting using conceptual models, 1. A
723 discussion of principles. *Journal of Hydrology*, **10**: 280-290.
- 724 Niel H, Paturol J E, Servat E. 2003. Study of parameter stability of a lumped
725 hydrologic model in a context of climatic variability, *Journal of Hydrology*, **278**:
726 213-230.

727 Peel M C, Chiew F H S, Western A W, McMahon T A. 2000. Extension of
728 unimpaired monthly stream flow data and regionalization of parameter values to
729 estimate stream flow in ungauged catchments. Report to National Land and Water
730 Resources Audit, Cent. For Environ. Appl. Hydrol., Univ. of Melbourne, Parkville,
731 Vic., Australia.

732 Perrin C., Oudin L., Anderassian V., Rojas-serna C., Michel C., and Mathevet T. 2007.
733 Impact of limited streamflow data on the efficiency and the parameters of
734 rainfall-runoff models. *Hydrological Sciences Journal*, **52**:1, 131-151.

735 Rind D, Rosenzweig C, Goldberg R. 1992. Modelling the hydrological cycle in
736 assessments of climate change, *Nature*, **358**: 119-120.

737 Priestley C H B, Taylor R J. 1972. On the assessment of the surface heat flux and
738 evaporation using large-scale parameters, *Monthly Weather Review*, **100**: 81-92.

739 Sankarasubramanian, A., Vogel, R.V., 2003. Hydroclimatology of the continental
740 United States, *Geophysical Research Letter*, **30**(7), 1363.
741 doi:10.1029/2002GL015937.

742 Segond, M. L., Wheater, H. S., Onof, C., 2007. The significance of spatial rainfall
743 representation for flood runoff estimation: A numerical evaluation based on the Lee
744 catchment, UK, *Journal of Hydrology*, **347**(1-2): 116-131.

745 Siriwardena L, Finlayson B L, McMahon T A. 2006. The impact of land use change
746 on catchment hydrology in large catchments: The Comet River, Central Queensland,
747 Australia, *Journal of Hydrology*, **326**: 199-214.

748 Smith M B , Koren V I, Zhang Z Y, Reed S M, Pan J J and Moreda F. 2004. Runoff
749 response to spatial variability in precipitation: an analysis of observed data, *Journal of*
750 *Hydrology*, **298**: 267-286.

751 Raupach M R. 2000. Equilibrium evaporation and the convective boundary layer,
752 *Boundary-Layer Meteorology*, **96**: 107-141.

753 Raupach M R, J M Kirby, D J Barrett, P R Briggs, H Lu and L Zhang. 2001. Balances
754 of water, carbon, nitrogen and phosphorus in Australian landscapes: 2. Model
755 formulation and testing, Tech. Rep. 41/01, CSIRO Land and Water, Canberra, ACT,
756 Australia.

757 Refsgaard J C, Storm B. 1996. Construction, calibration and validation of
758 hydrological models. In Abbott, M. B., and Refsgaard, J. C. (ed.) *Distributed*
759 *Hydrological Modelling*, Kluwer Academic Publishers, Netherlands, 50 pp.

760 Seibert, J., 2003. Reliability of model predictions outside calibration conditions,
761 *Nordic Hydrology*, **34**: 477-492.

762 Singh, R., Wageber, T., Vab Werkhoveb, K., Mann, M., and Crane, R. (2011). A
763 trading-space-for time approach to probabilistic continuous streamflow predictions in
764 a changing climate. *Hydrol. Earth Syst. Sci. Discuss.*, **8**, 6385-6417.

765 Uhlenbrook S, Seibert J, Leibundgut C, Rodhe A. 1999. Prediction uncertainty of
766 conceptual rainfall-runoff models caused by problems in identifying model
767 parameters and structure, *Hydrological Sciences – Journal des Sciences*
768 *Hydrologiques*, **44**(5): 779-797.

- 769 Vaze J, Post D A, Chiew F H S, Perraud J M, Viney N R, Teng J. 2010. Climate
770 non-stationarity – Validity of calibrated rainfall–runoff models for use in climate
771 change studies, *Journal of Hydrology*, **394**: 447-457.
- 772 Viney N, Vaze J, Chiew F, Perraud J. 2008. Regionalisation of runoff generation
773 across the Murray–Darling Basin using an ensemble of two rainfall–runoff models.
774 Paper presented at Water Down Under 2008, April 2008, Adelaide: Engineers
775 Australia.
- 776 Wagener, T., N. McIntyre, M. J. Lees, H. S. Wheater, and H. V. Gupta. 2003.
777 Towards reduced uncertainty in conceptual rainfall-runoff modeling: Dynamic
778 identifiability analysis, *Hydrol. Processes*, **17**, 455-476.
- 779 Wagener, T., M. Sivapalan, P. A. Troch, B. L. McGlynn, C. J. Harman, H. V. Gupta,
780 P. Kumar, P. S. C. Rao, N. B. Basu, and J. S. Wilson. 2010. The future of hydrology:
781 An evolving science for a changing world, *Water Resour. Res.*, **46**, W05301,
782 doi:10.1029/2009WR008906.
- 783 Widen-Nilsson E, Gong L, Halldin S, Xu C Y. 2009. Model performance and
784 parameter behavior for varying time aggregations and evaluation criteria in the
785 WASMOD-M global water balance model. *Water Resources Research*, **45**: W05418,
786 doi:10.1029/2007WR006695.
- 787 Wilby R L. 2005. Uncertainty in water resource model parameters used for climate
788 change impact assessment, *Hydrological Processes*, **19**: 3201-3219.
- 789 Xu C Y. 1999. Operational testing of a water balance model for predicting climate
790 change impacts, *Agricultural and Forest Meteorology*, **98**(9): 295-304.
- 791 Zhang L, Dawes W R, Walker G R. 2001. Response of mean annual
792 evapotranspiration to vegetation changes at catchment scale. *Water Resources
793 Research*, **37**: 701-708.
- 794 Zhang L, Hickel K, Dawes W R, Chiew F H S, Western A W, Briggs P R. 2004. A
795 rational function approach for estimating mean annual evapotranspiration, *Water
796 Resources Research*, **40**: W02502, doi:10.1029/2003WR002710.
- 797 Zhang L, Potter N, Zhang Y Q, Hickel K, Shao Q X. 2008. Water balance modeling
798 over variable time scales based on the Budyko framework: model development and
799 testing, *Journal of Hydrology*, **360**: 117-131.
- 800 Zhang Y Q, Chiew F H S, Zhang L, Leuning R, Cleugh H A. 2008. Estimating
801 catchment evaporation and runoff using MODIS leaf area index and the
802 Penman–Monteith equation, *Water Resources Research*, **44**: W10420,
803 doi:10.1029/2007WR006563.
- 804 Zhang Y Q, Chiew F H S, Zhang L, Li H X. 2009. Use of remotely sensed actual
805 evapotranspiration to improve rainfall–runoff modelling in southeast Australia,
806 *Journal of Hydrometeorology*, **10**, 969-980. doi: 10.1175/2009JHM1061.1.

807 **Table and Figure Captions**

808 **Table 1** Ranges of parameter values in DWBM (/ indicates dimensionless).

809

810 **Table 2** Ranges of parameters in the SIMHYD model (/ indicates dimensionless).

811

812 **Table 3** Summary results of the model calibration under different climatic conditions

813 (*i.e.* dry and wet periods).

814

815 **Table 4** Summary results of the model validation when calibrated under different

816 climatic conditions.

817

818 **Table 5** Percent of the catchments in which the model parameter distributions for a

819 dry and wet calibration period were significantly different ($p < 0.01$) under Monte

820 Carlo simulation. Also shown are the results for water-limited ($E_p/P > 1$) and

821 energy-limited ($E_p/P < 1$) catchments. For each model, the parameters are ranked from

822 the most sensitive to calibration conditions to least sensitive.

823

824

825

826

827

828

829

830 **Figure 1** Structure of the lumped dynamic water balance model (DWBM).

831

832 **Figure 2** Structure of the lumped daily rainfall–runoff model (SIMHYD).

833

834 **Figure 3** Location map of the 30 catchments used for this study.

835

836 **Figure 4** Annual historical precipitation of the Corang River catchment showing
837 estimation of 2 wet periods (A) and 2 dry periods (B) to represent different calibration
838 conditions.

839

840 **Figure 5 (a)** Percentage of model calibration tests with a NSE value greater than or
841 equal to a given NSE value. Similarly, **Figure 5 (b-c)** are corresponding plots of the
842 modified index of agreement (d_I), the water balance error (WBE), respectively.

843

844 **Figures 6 (a) and (d)** Percentage of model validation tests with a NSE value greater
845 than or equal to a given NSE value. Similarly, **Figures 6 (b) and (e)**, **Figures 6 (c)**
846 **and (f)** are corresponding plots of the modified index of agreement (d_I), the water
847 balance error (WBE), respectively.

848

849 **Figure 7** Probability density functions for 7 parameters of the SIMHYD model under
850 dry and wet calibration periods in catchments 110003 and 4021210.

851

852

853 **Figure 8** Probability density functions for 4 parameters of the DWBM model under
854 dry and wet calibration periods in catchments 110003 and 4021210.

855

856

857

858

859

860

861

862

863

864

865

866

867

868

869

870

871

872

873 **Tables and Figures**

874 **Table 1** Ranges of parameter values in DWBM (/ indicates dimensionless).

Parameter	Units	Description	Lower bound	Upper bound
α_1	/	retention efficiency	1	5
α_2	/	evapotranspiration efficiency	1	5
S_{max}	mm	soil water storage capacity	5	500
d	/	baseflow linear regression	0.01	1

875

876 **Table 2** Ranges of parameter values in the SIMHYD model (/ indicates
877 dimensionless).

Parameter	Units	Description	Lower bound	Upper bound
INSC	mm	interception store capacity	0.5	5.0
COEFF	mm	maximum infiltration loss	50	400
SQ	/	infiltration loss exponent	0	6.0
SMSC	mm	soil moisture store capacity	50	500
SUB	/	constant of proportionality in interflow equation	0	1
CRAK	/	constant of proportionality in groundwater recharge equation	0	1
K	/	baseflow linear regression parameter	0.003	0.3

878

879 **Table 3** Summary results of the model calibration under different climatic conditions
 880 (*i.e.* dry and wet periods).

Indicator	SIMHYD calibrated on dry period	SIMHYD calibrated on wet period	DWBM calibrated on dry period	DWBM calibrated on wet period
25th NSE	0.84	0.85	0.71	0.77
Median NSE	0.70	0.77	0.58	0.66
75th NSE	0.61	0.68	0.43	0.54
Average NSE	0.70	0.76	0.57	0.65
25th d_I	0.77	0.79	0.71	0.75
Median d_I	0.72	0.76	0.67	0.71
75th d_I	0.70	0.74	0.61	0.68
Average d_I	0.73	0.76	0.65	0.71
25th WBE	22	16	25	24
Median WBE	13	8	15	12
75th WBE	6	4	9	5
Average WBE	14	11	22	17

881

882

883

884

885

886

887

888

889

890

891

892

893

894 **Table 4** Summary results of the model validation when calibrated under different
 895 climatic conditions.

Model	Indicator	dry/dry	dry/wet	wet/dry	wet/wet
SIMHYD	25th NSE	0.72	0.74	0.68	0.77
	Median NSE	0.55	0.64	0.51	0.69
	75th NSE	0.42	0.44	0.41	0.55
	Average NSE	0.57	0.61	0.54	0.66
	25th d_I	0.74	0.78	0.74	0.78
	Median d_I	0.71	0.74	0.70	0.75
	75th d_I	0.66	0.70	0.63	0.72
	Average d_I	0.69	0.73	0.68	0.74
	25th WBE	34	30	39	23
	Median WBE	20	19	28	13
	75th WBE	14	8	16	7
	Average WBE	24	21	29	17
DWBM	25th NSE	0.56	0.65	0.51	0.72
	Median NSE	0.46	0.48	0.45	0.61
	75th NSE	0.34	0.35	0.30	0.42
	Average NSE	0.48	0.52	0.45	0.59
	25th d_I	0.69	0.73	0.68	0.74
	Median d_I	0.65	0.69	0.63	0.70
	75th d_I	0.58	0.64	0.56	0.66
	Average d_I	0.62	0.68	0.61	0.69
	25th WBE	35	29	53	25
	Median WBE	22	20	33	18
	75th WBE	15	12	18	11
	Average WBE	27	23	36	19

896

897

898

899

900

901

902

903

904

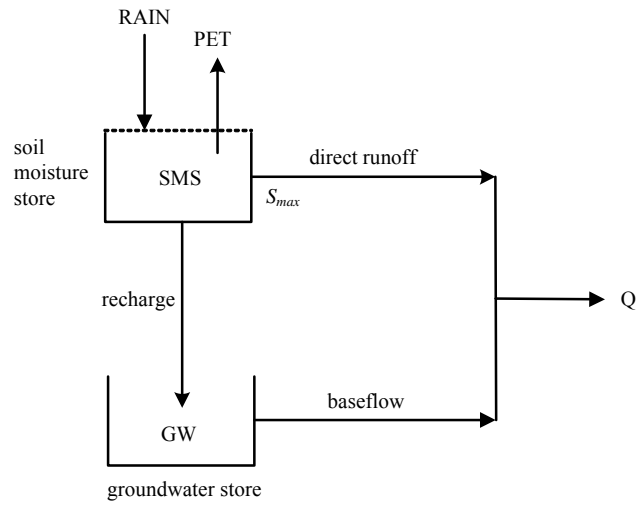
905

906 **Table 5** Percent of the catchments in which the model parameter distributions for a
 907 dry and wet calibration period were significantly different ($p < 0.01$) under Monte
 908 Carlo simulation. Also shown are the results for water-limited ($E_p/P > 1$) and
 909 energy-limited ($E_p/P < 1$) catchments. For each model, the parameters are ranked from
 910 the most sensitive to calibration conditions to least sensitive.

Model	Parameter	Percent of catchments	Percent of water-limited catchments	Percent of energy-limited catchments
SIMHYD	SUB	63	81	43
	SMSC	60	75	43
	SQ	53	56	50
	CRAK	50	63	36
	K	37	31	43
	COEFF	33	38	29
	INSC	10	13	7
DWBM	α_1	67	81	50
	S_{max}	63	75	50
	d	47	63	29
	α_2	23	25	21

911

912



Model parameters and description

- α_1 retention efficiency
- α_2 evapotranspiration efficiency
- S_{max} soil water storage capacity (mm)
- d baseflow linear regression

913

914 **Figure 1** Structure of the lumped dynamic water balance model (DWBM).

915

916

917

918

919

920

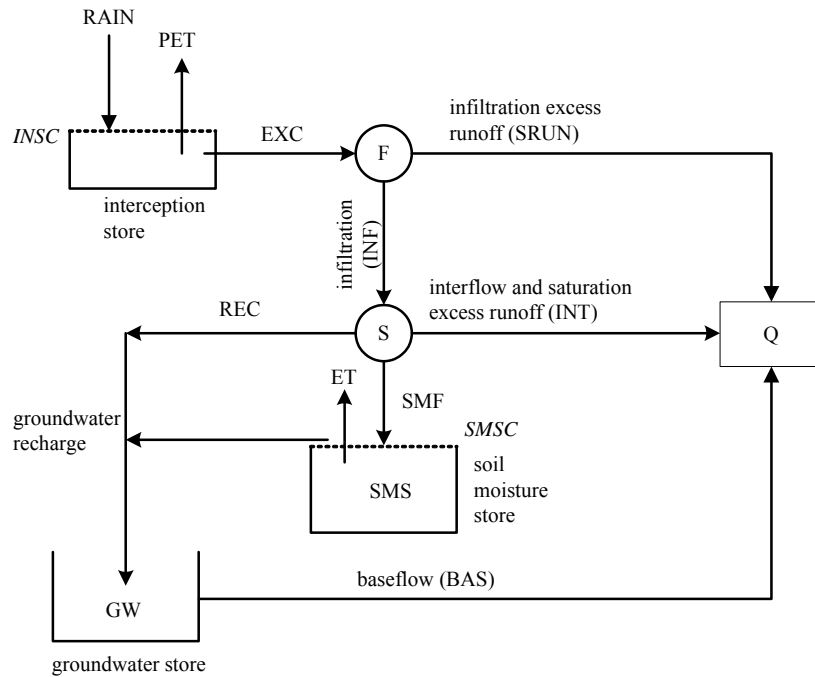
921

922

923

924

925



PET = areal potential evapotranspiration (input data)
 $EXC = RAIN - INSC$, $EXC > 0$
 $INF = \text{lesser of } \{ COEFF \exp(-SQ \times SMS/SMSC), EXC \}$
 $SRUN = EXC - INF$
 $INT = SUB \times SMS/SMSC \times INF$
 $REC = CRAK \times SMS/SMSC \times (INF - INT)$
 $SMF = INF - INT - REC$
 $ET = \text{lesser of } \{ 10 \times SMS/SMSC, PET \}$
 $BAS = K \times GW$

Model parameters and description

- INSC interception store capacity (mm)
- COEFF maximum infiltration loss (mm)
- SQ infiltration loss exponent
- SMSC soil moisture store capacity (mm)
- SUB constant of proportionality in interflow equation
- CRAK constant of proportionality in groundwater recharge equation
- K baseflow linear recession parameter

927

928 **Figure 2** Structure of the lumped daily rainfall-runoff model SIMHYD.

929

930

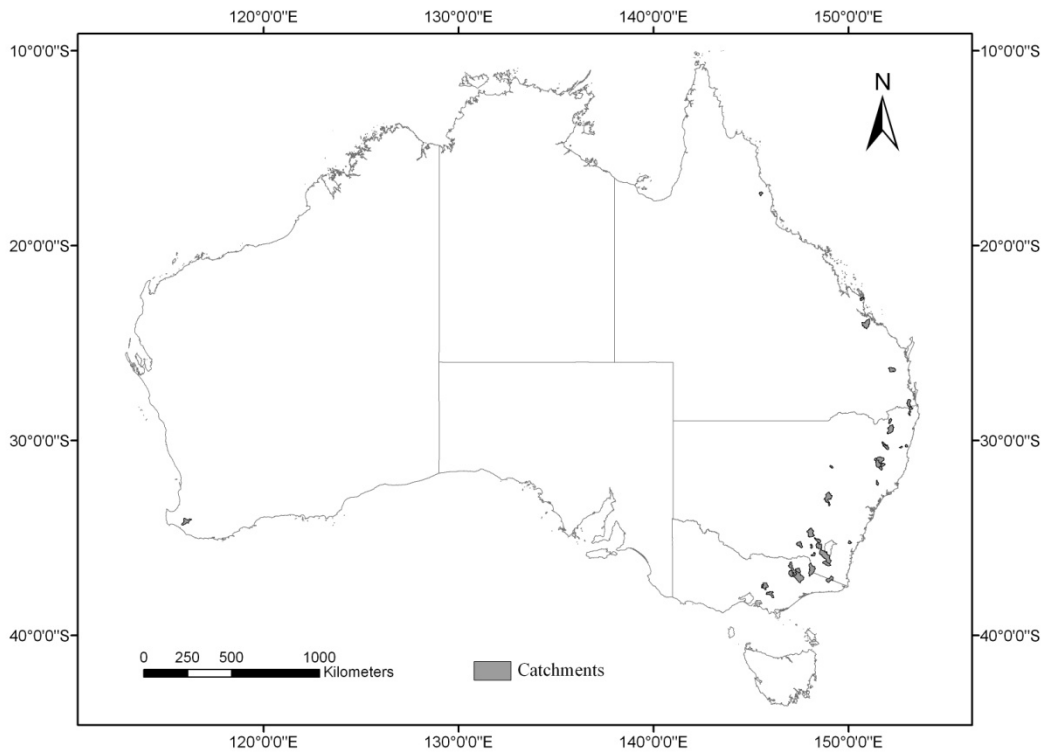
931

932

933

934

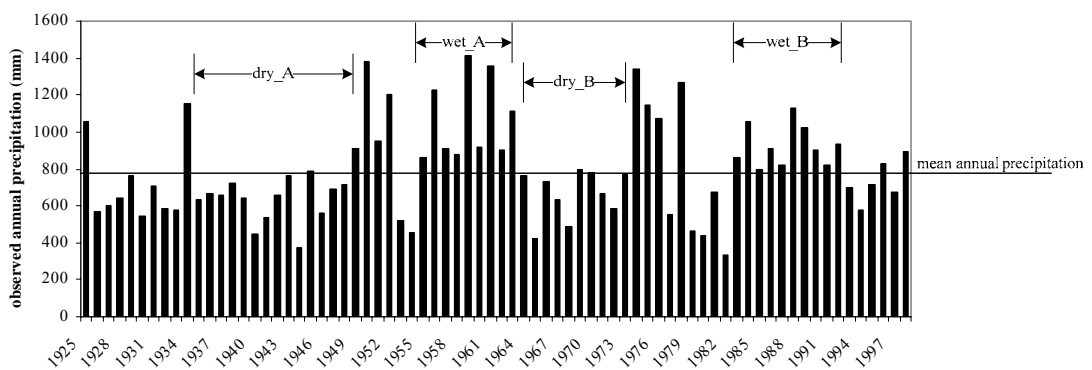
935



936

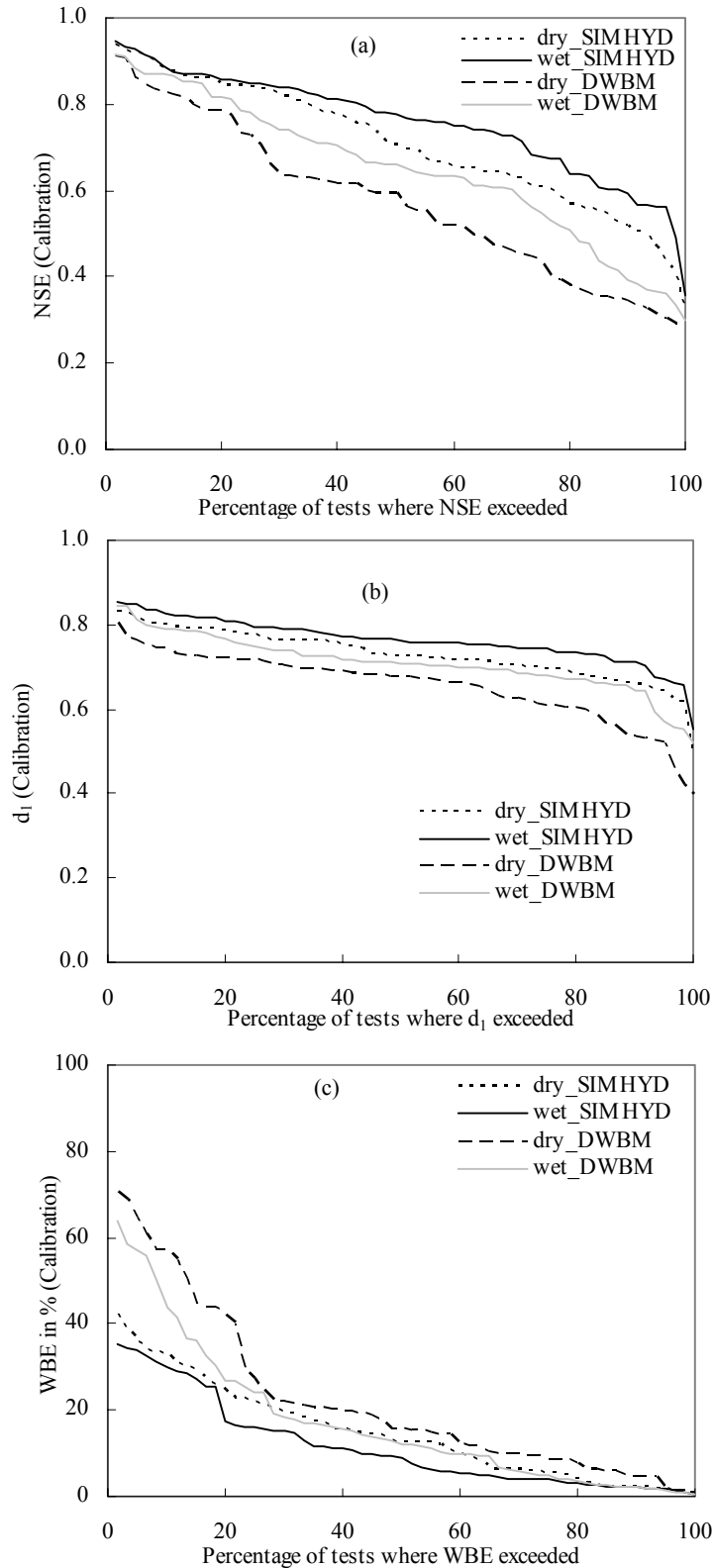
937 **Figure 3** Location map of the 30 catchments used for this study.

938



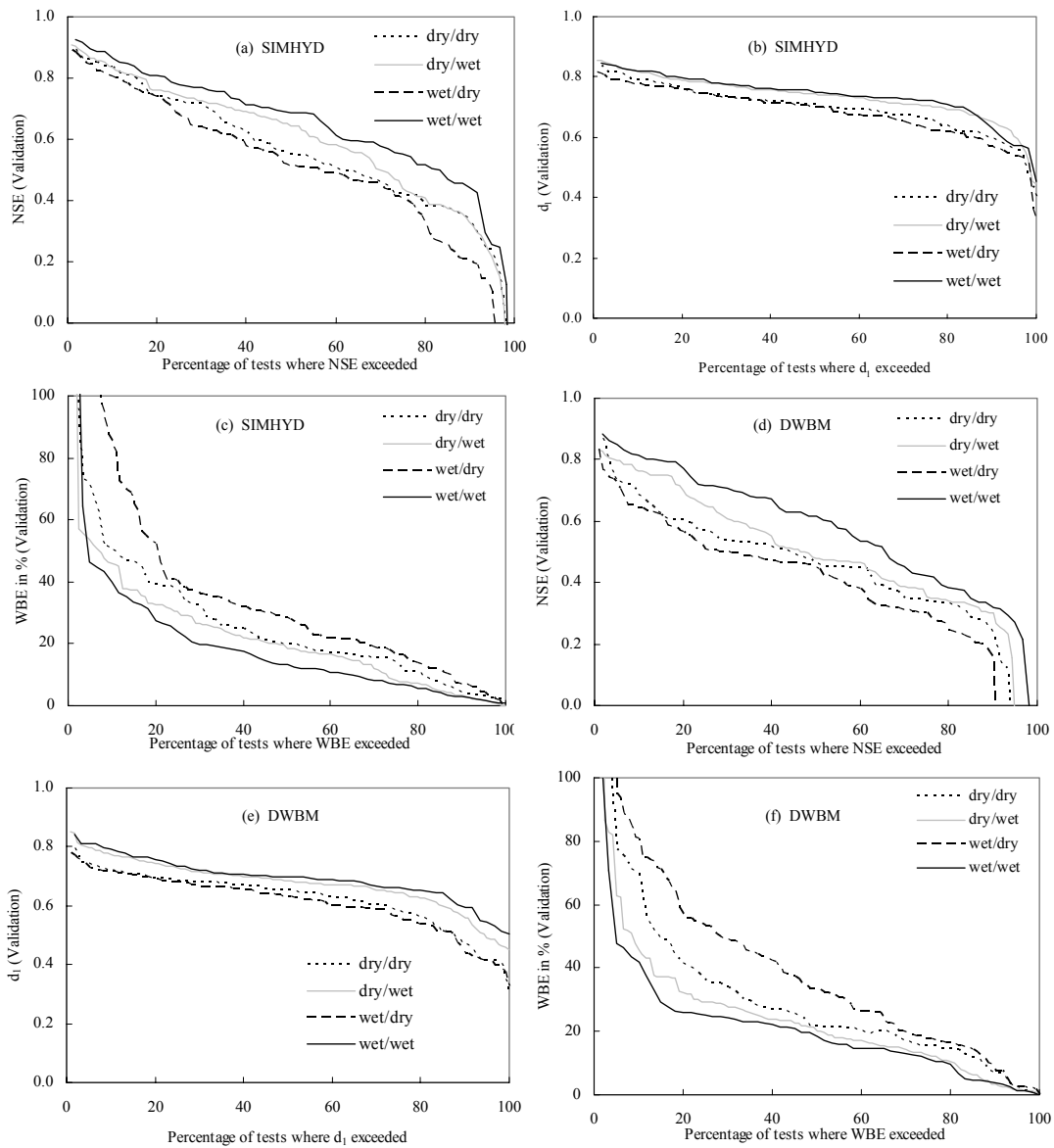
939

940 **Figure 4** Annual historical precipitation of the Corang River catchment showing
941 estimation of 2 wet periods (A) and 2 dry periods (B) to represent different calibration
942 conditions.



943

944 **Figure 5 (a)** Percentage of model calibration tests with a NSE value greater than or
 945 equal to a given NSE value. Similarly, **Figure 5 (b-c)** are corresponding plots of the
 946 modified index of agreement (d_1) and the water balance error (WBE), respectively.

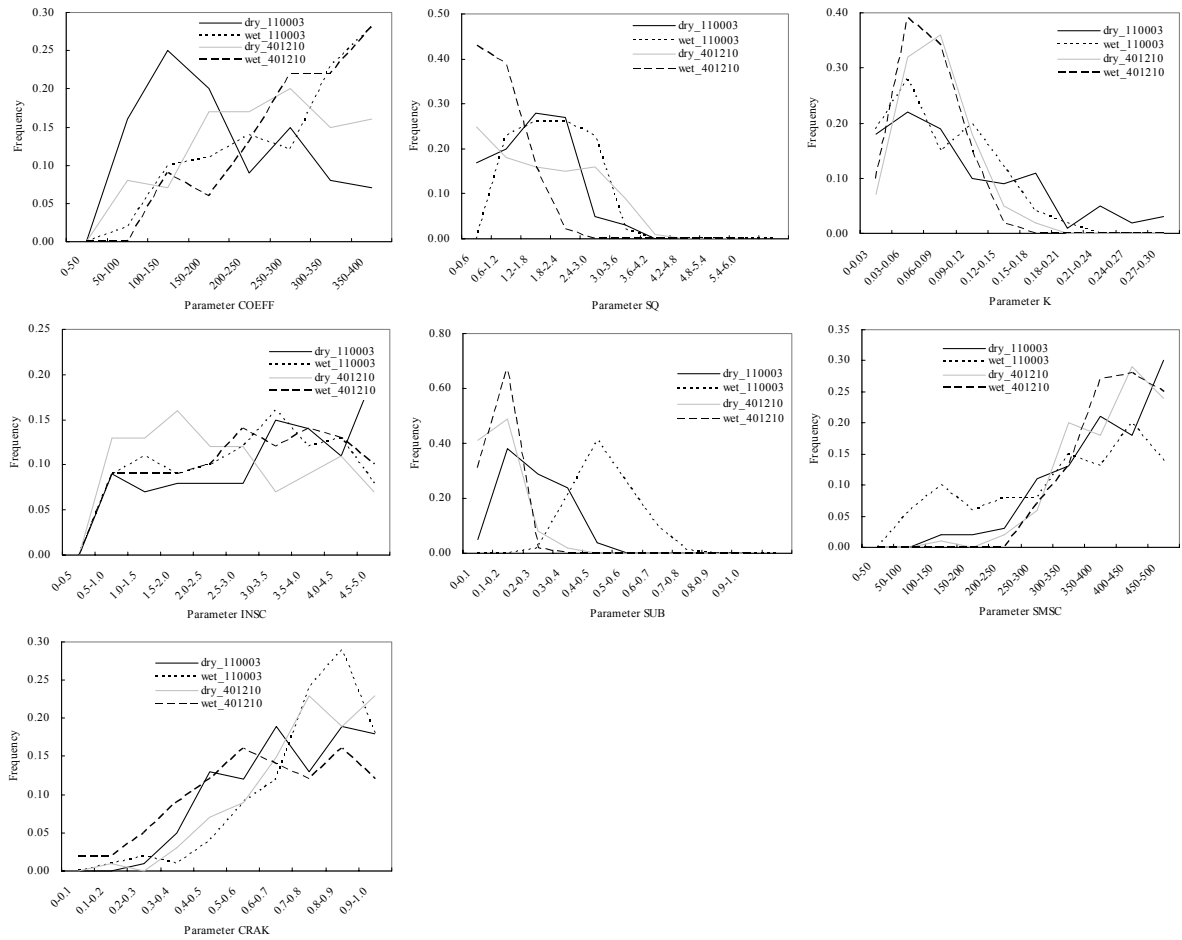


948

949

950 **Figures 6 (a) and (d)** Percentage of model validation tests with a NSE value greater
 951 than or equal to a given NSE value. Similarly, **Figures 6 (b) and (e), Figures 6 (c)**
 952 **and (f)** are corresponding plots of the modified index of agreement (d_1), the water
 953 balance error (*WBE*), respectively.

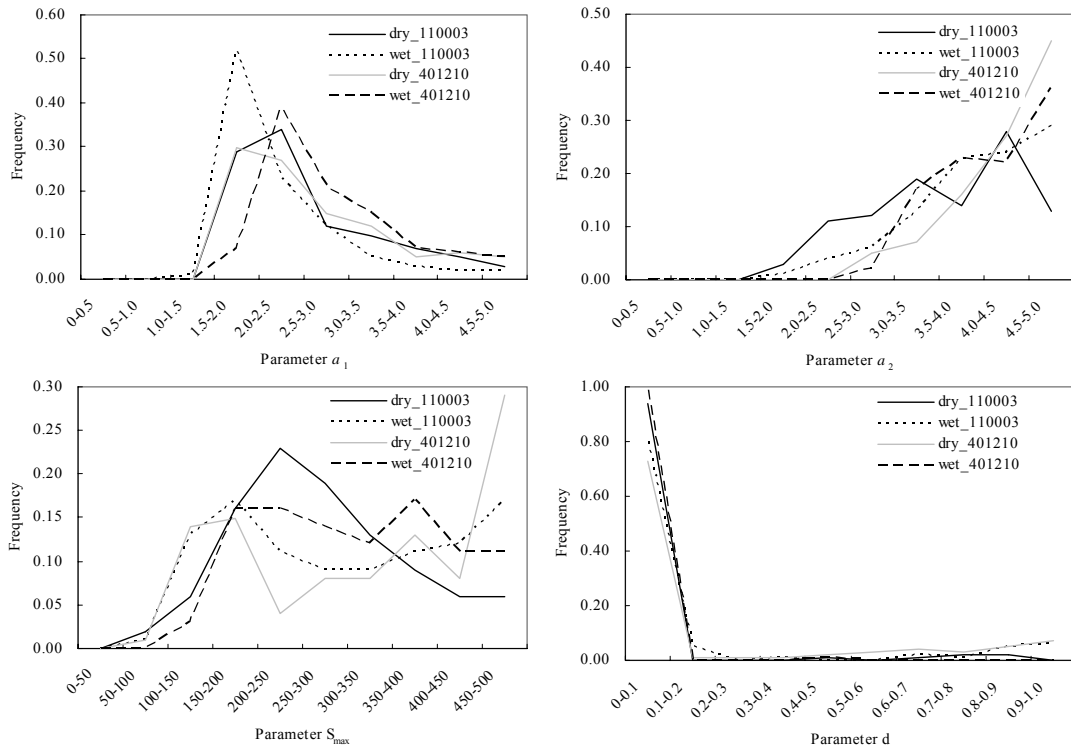
954



955

956 **Figure 7** Probability density functions for 7 parameters of the SIMHYD model under

957 dry and wet calibration periods in catchments 110003 and 4021210.



958

959 **Figure 8** Probability density functions for 4 parameters of the DWBM model under

960 dry and wet calibration periods in catchments 110003 and 401210.